Two-dimensional electron gas in a linearly varying magnetic field: Quantization of the electron and current density

E. Hofstetter, J. M. C. Taylor, and A. MacKinnon
Blackett Laboratory, Imperial College, London SW7 2BZ, United Kingdom
(Received 25 August 1995)

We have developed methods to calculate dispersion curves (analytically, in the simpler cases) from which we are able to derive the spatial distribution of electron and current densities. We investigate the case where the magnetic field varies linearly with position and the results provide useful insights into the properties of this and other field distributions. We consider a spin as well as a confining electrostatic potential. We show that the electron and the current density exhibit a very rich structure related to the quantization of the energy. Moreover, there is a direct contribution to the current density due to the spin, which could be of interest in relation to the spin-polarized current.

I. INTRODUCTION

A two-dimensional electron gas (2DEG) in a magnetic field has proved to be an extremely rich subject for theoretical and experimental investigation.[1] For example, considerable effort has been devoted to the study of the integral and fractional quantum Hall effects (I and FQHE), transport properties, and edge states.[2] Except in a few cases,[3–5] however, the magnetic field considered was homogeneous. In this paper, we address the problem of a magnetic field varying linearly with the position added to an underlying homogeneous field. This is of relevance, because in real systems (a) a constant magnetic field is not always attainable, and (b) an inhomogeneous field may be desired, and produced, for example, by means of magnetic gates (gates of superconducting or ferromagnetic materials). Another interesting point is that in the composite fermion (CF) theory,[6,7] which is used to describe the FQHE, the electron-electron interaction, necessary for the appearance of the FQHE, is incorporated into an effective magnetic field via a singular gauge transformation. The result is a system of noninteracting quasiparticles carrying a fictitious magnetic flux in an inhomogeneous effective magnetic field. It must be stressed that in the CF case, the effective magnetic field is a function of the local electron density and should be calculated self-consistently, in contrast to the case that we consider in this paper. Nevertheless, a better understanding of the properties of a simple noninteracting electron gas in an inhomogeneous field might bring useful insights into CF theory.

II. MODEL

To investigate the electronic properties of a noninteracting electron gas in a linearly varying magnetic field, we consider the following Hamiltonian:

$$H=\frac{1}{2m^*}(\mathbf{p}-e\mathbf{A})^2-\frac{g^*e}{2m_e}\mathbf{SB}+V_c, \tag{1}$$

where $\mathbf{A}=(\frac{1}{2}B_1y^2+B_0y,0,0)$, $\mathbf{B}=-(0,0,B_1y+B_0)$, the confining potential due to the walls $V_c(y)=\beta\{\exp[\alpha/y_e(y-y_e)]+\exp[-\alpha/y_e(y+y_e)]\}$, y_e is the position of the edge of the system, $\mathbf{S}$ is the spin operator. The parameters α and β allow the shape of the potential to change continuously from very sharp to very smooth, which can modify the properties of the system.[7,8] By solving

$$\left(\frac{1}{2m^*}(\mathbf{p}-e\mathbf{A})^2-\frac{g^*e}{2m_e}\mathbf{SB}+V_c\right)\chi(x,y)=E\chi(x,y), \tag{2}$$

we can obtain the electron density

$$\rho(x,y)=\sum_{\text{states}}\chi^*(x,y)\chi(x,y), \tag{3}$$

where we sum over all states with energy $E\leqslant E_F$, and the current density for a state n,[9]

$$\mathbf{j}^{(n)}(x,y)=\frac{e}{m^*}\,\mathrm{Re}[\chi_n^*(x,y)(\mathbf{p}-e\mathbf{A})\chi_n(x,y)]+\frac{g^*e}{2m_e}\nabla\times[\chi_n^*(x,y)\mathbf{S}\chi_n(x,y)]. \tag{4}$$

As a result of our choice of $\mathbf{A}$ and $\mathbf{B}$, the symmetry of the Hamiltonian allows us to write the wave function as $\chi(x,y)=\mathrm{e}^{ik_xx}\psi(y)$, where k_x is a good quantum number, and we then obtain the one-dimensional Schrödinger equation:

$$\left[\frac{p_y^2}{2m^*}+\frac{1}{2m^*}(\hbar k_x-eA_x)^2-\frac{g^*e\hbar s}{2m_e}B_z+V_c\right]\psi(y)=E\psi(y), \tag{5}$$

with $s=\pm0.5$. Equation (5) then enables us to derive the dispersion curves $E_n(k_x)$, and to rewrite the electron density as

$$\rho(y)=\sum_n\sum_{k_x}\psi_n^*(y)\psi_n(y), \tag{6}$$

and the current density for one state n and a fixed k_x as

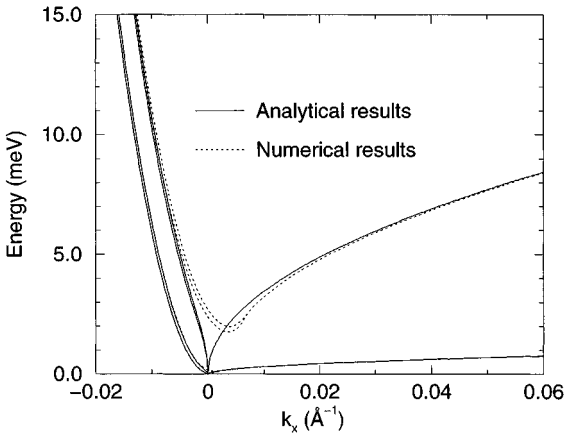

FIG. 1. Dispersion curves obtained analytically compared with numerical results. $V_c=0$, $B_1=1$ G/Å, and $B_0=0$. The curves plotted correspond to the levels $n=0,1,10,11$.

$$j_x^{(n)}(y)=\frac{e}{m^*}[\psi_n^*(y)(\hbar k_x-eA_x)\psi_n(y)] + \frac{g^*e\hbar s}{2m_e}\frac{\partial[\psi_n^*(y)\psi_n(y)]}{\partial y}, \tag{7}$$

both now solely functions of y. Due to the symmetry of the system, there is a current density only along the x axis. Integrating over y will give the total current I_x^n carried, for a fixed k_x by the state n and summing over n and k_x the total current I_x.

III. METHOD

Starting from Eq. (5), the Hamiltonian can be written as

$$\left[\frac{p_y^2}{2m^*}+\frac{m^*\omega_1^2}{8}y^4+\frac{m^*\omega_1\omega_0}{2}y^3+\left(\frac{m^*\omega_0^2}{2}-\frac{\hbar k_x\omega_1}{2}\right)y^2 + \left(\frac{e\hbar sB_1}{m_e}-\hbar k_x\omega_0\right)y+\left(\frac{g^*e\hbar sB_0}{2m_e}+\frac{\hbar^2k_x^2}{2m^*}\right) + V_c(y)\right]\psi(y)=E\psi(y), \tag{8}$$

with $\omega_0=eB_0/m^*$ and $\omega_1=eB_1/m^*$. For what follows, it is useful to introduce the dimensionless variable $\hat{y}=(\hbar^{-1}m^*\omega_1)^{1/3}y$ and $\hat{p}=(m^*\omega_1\hbar^2)^{-1/3}p$, which yields for (8),

$$\left(\frac{p_{\hat{y}}^2}{2m'}+a\hat{y}^4+b\hat{y}^3+c\hat{y}^2+d\hat{y}+e+V_c(\hat{y})\right)\psi(\hat{y})=E\psi(\hat{y}), \tag{9}$$

with $m'=m^*/(m^*\omega_1\hbar^2)^{2/3}$ and a,b,c,d,e now given in units of energy. Although in some simplified cases it is possible to obtain analytical results, as we will see below, there is, in general, no way to find the analytical solution of Eq. (9), and, therefore, we have to resort to numerical calculations. Equation (9) can be solved by expanding $\psi(\hat{y})$ in terms of oscillator functions, $\phi_n(\hat{y})=\mathrm{H}_n(\hat{y})\mathrm{e}^{-\hat{y}^2/2}$, where H_n is a Hermite polynomial, and then by numerically diagonalizing the corresponding secular equation,

$$\mathrm{Det}|H_{kn}-E\delta_{kn}|=0. \tag{10}$$

Using the properties of the Hermite polynomials, all of the matrix elements $\langle\phi_k|H|\phi_n\rangle$ can be calculated analytically (Appendix), which greatly improves the diagonalization method. However, before starting with the numerical calculations, we can try an analytical approach to Eq. (8) in the simplified case where $B_0=0$ and $V_c=0$. We then have

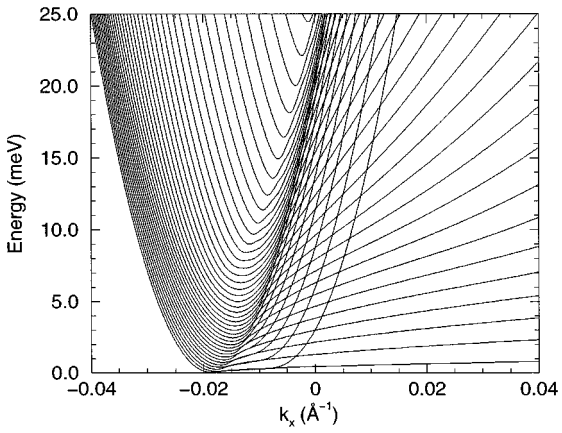

FIG. 2. Dispersion curves with $V_c\neq0$, $B_1=1$ G/Å, and $B_0=0.5\times10^4$ G.

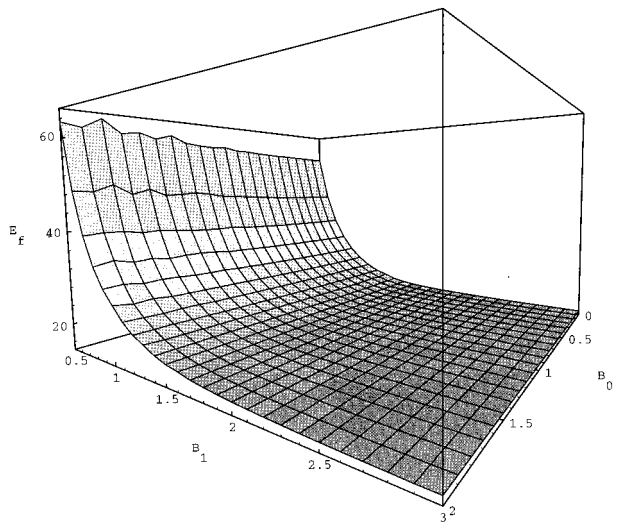

FIG. 3. Fermi energy, as a function of the magnetic field **B**.

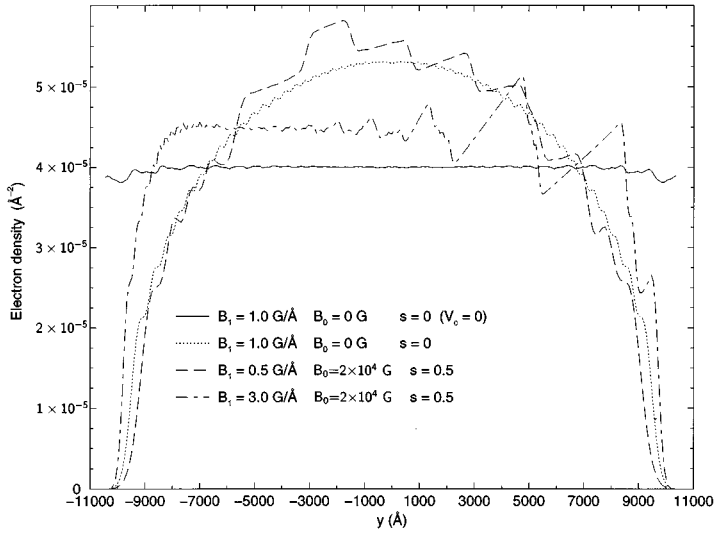

FIG. 4. Electron densities for different magnetic fields. The solid line corresponds to the case without an external confining potential.

$$\left[\frac{p_y^2}{2m^*}+\frac{\hbar^2}{2m^*}\left(\frac{e^2B_1^2}{4\hbar^2}y^4-\frac{eB_1}{\hbar}k_xy^2+\frac{g^*eB_1m^*s}{\hbar m_e}y+k_x^2\right)\right]\psi(y)=E\psi(y). \tag{11}$$

We choose two regimes for which $B_1\neq 0$: (a) $k_x<0$, single well potential (SWP), near $B=0$, and (b) $k_x>0$, double well potential (DWP), near $B=\pm B_1|\sqrt{2\hbar k_x/eB_1}|$. We expand parabolically around the minima of the effective potential and obtain harmonic oscillator equations, which we solve analytically. The expressions obtained for the energy are

$$\text{SWP:}\quad E_n=\frac{\hbar^2}{2m^*}\left[k_x^2+(2n+1)\sqrt{\frac{k_xeB_1}{\hbar}}-\frac{eB_1\eta^2}{\hbar k_x}\right], \tag{12}$$

$$\text{DWP:}\quad E_n=\frac{\hbar^2}{2m^*}\left[(2n+1)\sqrt{\frac{2k_xeB_1}{\hbar}}-\frac{eB_1\eta^2}{2\hbar k_x}\pm 2\eta\sqrt{\frac{2k_xeB_1}{\hbar}}\right], \tag{13}$$

where $\eta=g^*m^*s/2m_e$. From here it is straightforward to derive the group velocity $(1/\hbar dE_n/dk_x)$ for the state n as

$$\text{SWP:}\quad v_x=\frac{\hbar}{m^*}\left[k_x+\frac{eB_1\eta^2}{2\hbar k_x^2}+(2n+1)\sqrt{\frac{eB_1}{16\hbar k_x}}\right], \tag{14}$$

$$\text{DWP:}\quad v_x=\frac{\hbar}{m^*}\left[\frac{eB_1\eta^2}{4\hbar k_x^2}+(2n+1)\sqrt{\frac{eB_1}{8\hbar k_x}}\pm\eta\sqrt{\frac{eB_1}{2\hbar k_x}}\right]. \tag{15}$$

IV. RESULTS

In the following calculations, the system we consider corresponds to an ideal slab of GaAs/Al_xGa_{1-x}As heterostructure filled with an ideal 2DEG. The effective electron mass is $m^*=0.067m_e$, the effective g factor is $g^*=-0.44$, the electron density 4×10^{-5} Å^{-2}, and the sample has width, when $V_c\neq 0$, $2y_e=2\times10^4$ Å and length $L\gg 1$ with periodic boundary conditions along x.

The numerical and the analytical results [Eqs. (12),(13)] for the case when $V_c=0$, $B_1=1$ G/Å, and $B_0=0$ are reported in Fig. 1. We can see that the agreement is very good, except around $k_x=0$, where the method breaks down. Al-

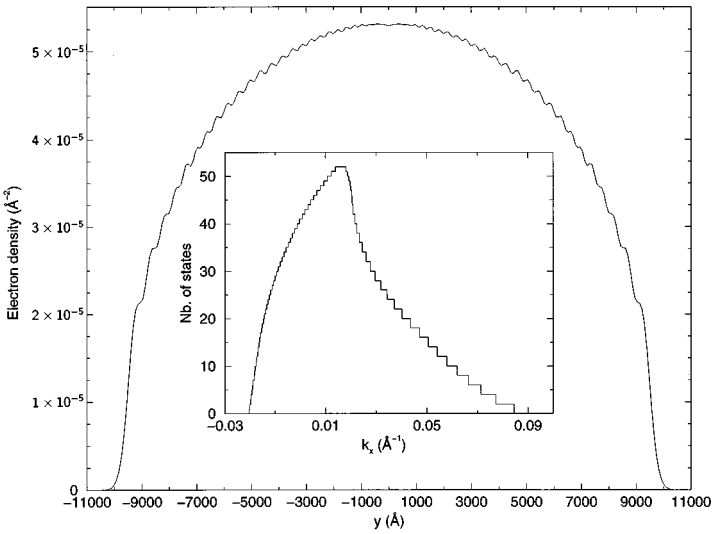

FIG. 5. Electron density $\rho(y)$ for $B_1=1$ G/Å and $B_0=0$. The inset shows the number of states, as a function of k_x. The number of oscillations in $\rho(y)$ corresponds to the number of states.

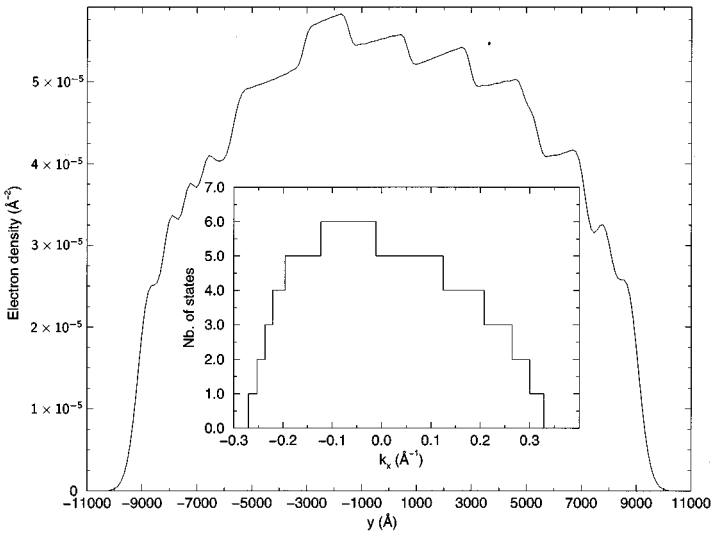

FIG. 6. Same as Fig. 5, but with $B_1=0.5$ G/Å and $B_0=2\times10^4$ G.

though it is possible to obtain useful information from analytical calculations, they do not allow us to derive complete dispersion curves and hence the electron or current densities. Moreover, we are interested in taking into account the effects of a confining potential V_c, but this cannot be included in our analytical approach. We then have to use a numerical approach.

So, we start with the same model system configuration as above, but this time with $V_c\neq0$ and $B_0=0.5\times10^4$ G. We chose $\alpha=100$ and $\beta=50$, which correspond to quite a sharp confining potential. The dispersion curves are plotted in Fig. 2. The degeneracy of the energy levels is completely removed and the structure appearing in the dispersion curves is due to the breaking of the y symmetry in the Hamiltonian. It is interesting to note that some similar features were observed in the case of a curved 2DEG in a constant magnetic field.[10] Having E_n and ψ_n, we can now calculate $j_x^{(n)}(y)$ and $\rho(y)$, but to do this we need the Fermi energy E_F. This can be obtained by minimizing the total energy with the constraint that the number of electrons N is constant with N given by

$$N=\frac{1}{2\pi}\sum_n \int_{k_{x1}^{(n)}}^{k_{x2}^{(n)}} dk_x^{(n)}, \tag{16}$$

where $\{k_{xi}^{(n)}\}$ are the parameters we vary to minimize the energy. As we might expect, E_F does not depend on k_x but, in contrast to the assumption in Ref. 3, it is not independent of the magnetic field. This is shown in Fig. 3, where E_F has been calculated for various values of B_1 and B_0. This dependence is due, in the absence of external leads, to the walls, which can be seen by the fact that when B_1, which in contrast to B_0 removes the degeneracy of the states and gives rise to an effective confining potential, increases, E_F becomes independent of the magnetic field.

Using E_F, we can now calculate the electron density $\rho(y)$. In Fig. 4, $\rho(y)$ is plotted for different values of B_1 and B_0. We see that with an external confining potential ($V_c\neq0$) $\rho(y)$ is not constant; it can have quite a rich structure with local charging effects. Moreover, when $B_0\neq0$, $\rho(y)$ becomes asymmetric in y. It has to be noted that in the case $V_c=0$ $\rho(y)$ is constant, the oscillations on the left and right hand sides of the graphic are only a numerical effect, due to

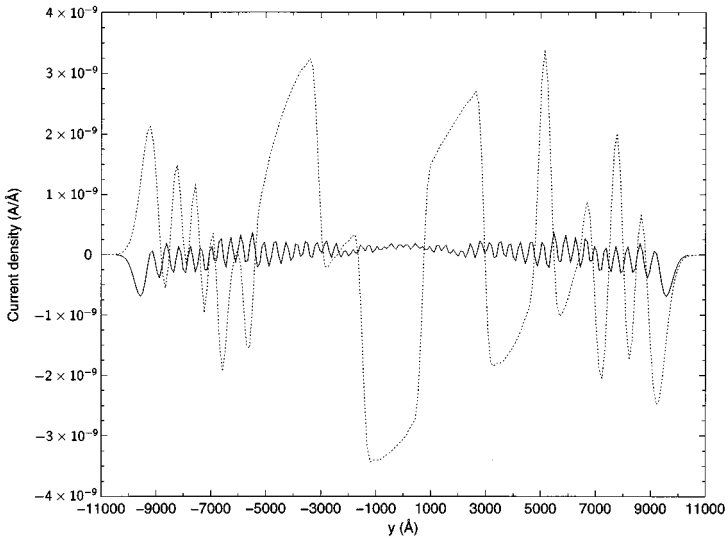

FIG. 7. Current density for two different magnetic fields. — : $B_1=1$ G/Å, $B_0=0$; and $\cdots$: $B_1=0.5$ G/Å, $B_0=2\times10^4$ G.

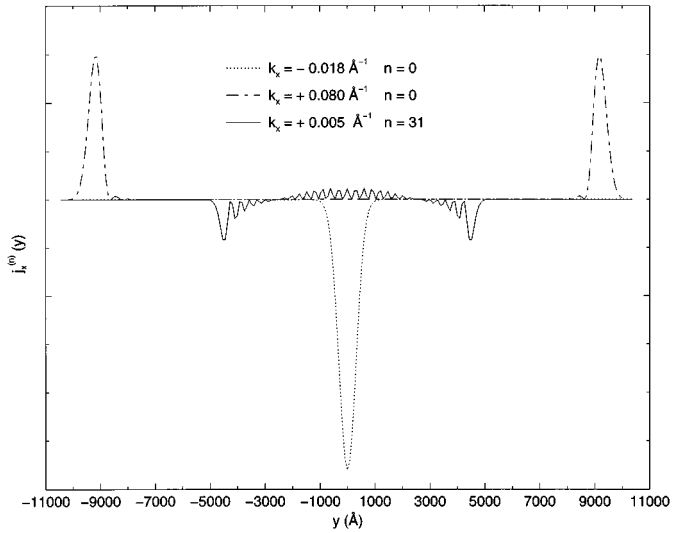

FIG. 8. Current density calculated for a fixed k_x and a fixed n. For $k_x=-0.018$ Å^{-1} ($\cdots$), $k_x=0.08$ Å^{-1} (-··-), and $n=0$, the movement of the electron is well defined by its classical orbits (edge and snake orbits). Around $k_x=0$, here $k_x=0.005$ Å^{-1} and $n=31$ (—), the situation is more complicated. The density of current can be positive *and* negative, as a function of y.

the fact that in this case one should use a larger set of ϕ_n for the expansion of ψ. But, for $V_c\neq 0$, the structure of $\rho(y)$ can be explained in the following way. When the number of states as a function of k_x is plotted, a discontinuous curve, due to the quantization of the energy, is obtained. Although there is no simple relation between the k_x space and the real space, as for a homogeneous magnetic field, the number of oscillations of the electron density is the same as the number of steps in the discontinuous curve and then is indeed a consequence of the energy quantization.

This can be seen in Figs. 5 and 6. The next step now is, by means of Eq. (7), to calculate the total current density given by

$$j_x(y)=\sum_{\text{states}} j_x^{(n)}(y), \tag{17}$$

where the sum runs over all the states with $E\leqslant E_F$. In Fig. 7 are reported the current densities for different magnetic fields disregarding first the part due to the spin. One sees that the shape of the current density is much more subtle than might be expected from semiclassical approximations. Actually considering $j_x^{(n)}(y)$ for $|k_x|\gg 0$ or, in other words for the largest k_x close to the Fermi energy, the movement of the electron can be described by its classical orbits (drifting orbits along the edge and snake orbits in the opposite direction along the line where $B\simeq 0$). For smaller k_x, however, the states tunneling between the two wells, but mainly the ones of energy above the central maximum of the double well, are very important and their contribution cannot be overlooked. In fact $j_x^{(n)}(y)$, after summing over all n and k_x, turns out to be very small for the case, where $B_0=0$ for all y. Different $j_x^{(n)}(y)$ are reported in Fig. 8. For $k_x=-0.018$ Å^{-1}, $k_x=0.08$ Å^{-1} and $n=0$ the movement of the electron is well defined by its classical orbits (edge and snake orbits). But around $k_x=0$ and, for example, here $n=31$, the situation is more complicated. An interesting point is that now the current density for one state can be positive *and* negative as a function of y. Moreover, we see that the positive part is located in y, where the density of current flows in the other direction, due to the presence of the snake orbits. The same kind of phenomena appears with edge orbits. This can be understood by considering the first term $\hbar k_x - \frac{1}{2}eB_1y^2-eB_0y$ in Eq. (7). It is easy to imagine that when summing the current density over all the different states, the

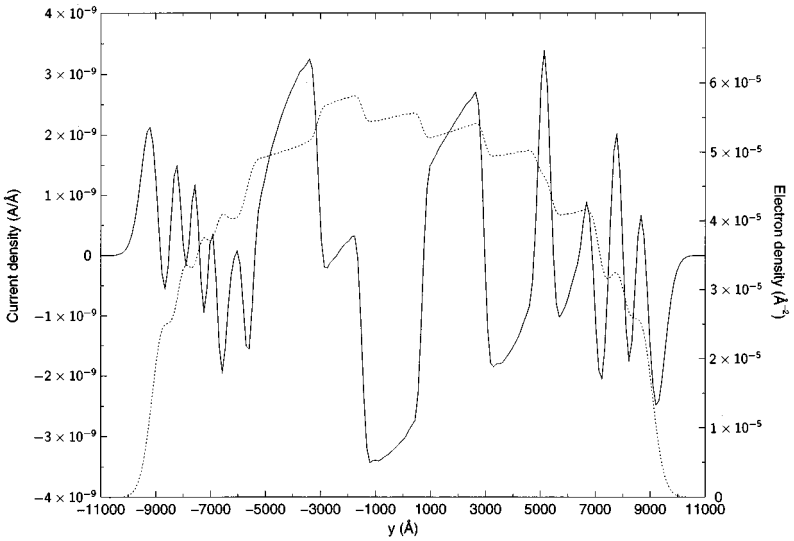

FIG. 9. Total density of current (sum over all states with $E\leqslant E_F$) for $B_1=0.5$ G/Å, $B_0=2\times 10^4$ G. The density of current (—) oscillates between positive and negative ''channels,'' as a function of the electron density ($\cdots$).

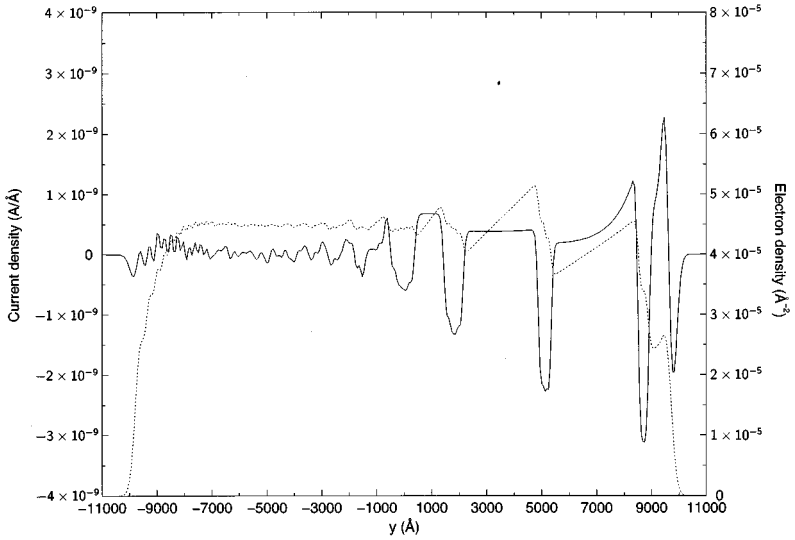

FIG. 10. Same as Fig. 9, but with $B_1=3\text{G/Å}$, $B_0=2\times10^4$ G.

result is rather different from what we might expect from the consideration of the simple classical picture of the orbits. It has to be noted that although the current density can be positive and negative as a function of y, the group velocity $v_g=\int dy j_x^{(n)}(y)$ has a well defined sign and has been verified from the dispersion curves by means of the relation $v_g=1/\hbar dE_n/dk_x$. In order to get a better understanding of the shape of the current density, we have plotted together the electron and the current densities in Figs. 9 and 10. The density of current oscillates between positive and negative ''channels,'' as a function of the electron density, and then is a reflection of the quantization of the energy. It is interesting to note that in the study of the FQHE, there is also the appearance of channels, which can be seen there as alternating strips of compressible and incompressible fluid.[8,11] When $B_0\neq0$, the current density increases with B_0 and flows in opposite directions on both sides of the sample when B_0 is large enough compared to B_1, or in other words, when B_0 is large enough to overcome the effective confining potential due to B_1, so that the electrons are confined by the external confining potential V_c. Moreover, the current density becomes asymmetric.

Until now only the first term in Eq. (7) has been considered, but there is a second term containing the derivative of the electron density and which is directly related to the presence of the spin for the electron. Because, as we have seen above, the electron density displays a very rich structure, one can expect some contribution to the current density, due to the spin of the electron. This is shown in Figs. 11 and 12. Although the part due to the spin is smaller than the first term in Eq. (7), it is nevertheless noticeable. This could imply some interesting phenomena in relation to spin-polarized currents. The problem is that the ''channels'' are more or less at the same position for spin up or down, which makes it quite difficult to distinguish between both spin directions. On the other hand, many parameters can be varied, such as the magnetic field, the width of the system, or the external confining potential, which may allow us to find a suitable system configuration for the production of polarized currents.

Finally, it has to be stressed that all the discussion above concerned the current density. Although this quantity is nonzero and has a rich structure, it does not imply that the net current $I_x=\Sigma_{k_x}\int j_x(y)dy$ is nonzero. In fact, as our calcula-

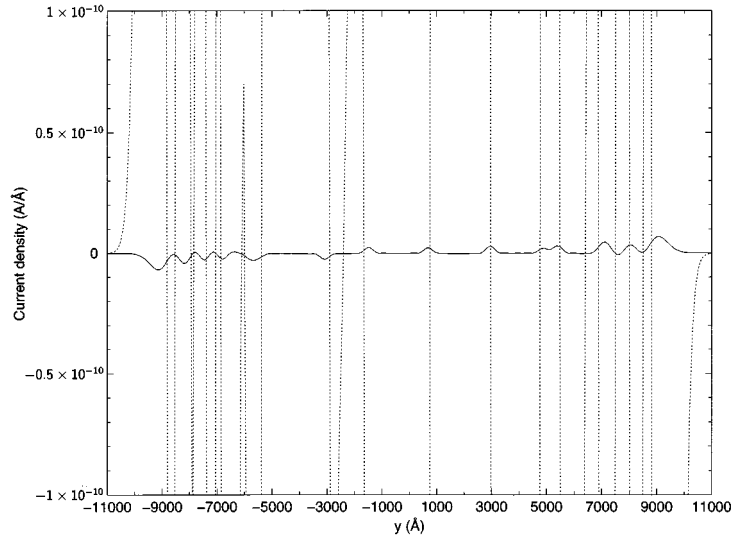

FIG. 11. Contribution due to the spin to the current density. The dotted line is the other contribution in Eq. (7) to the current density. $B_1=0.5$ G/Å, $B_0=2\times10^4$ G.

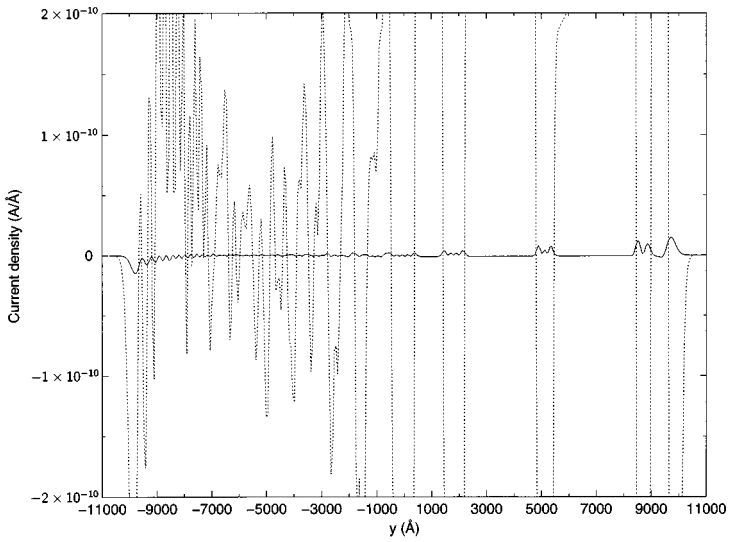

FIG. 12. Same as Fig. 11 but with $B_1=3$ G/Å, $B_0=2\times10^4$ G.

tion showed, E_F is independent of k_x, which means there is no difference of potential across our system and thus no net current.

V. CONCLUSIONS

In this work, we have studied the effect of a linear magnetic field in a 2DEG. In certain simplified cases, we were able to carry out some analytical calculations and to derive the dispersion curves $E_n(k_x)$ for quite a large range of $k_x \neq 0$. These results were found to be in very good agreement with our numerical results. In the general case with an external confining potential, we carried out numerical calculations. We derived the whole of the dispersion curve and using it, we calculated the electron and current densities. It is worthwhile noting that for this calculation, we need to consider the states for $k_x>0$, *as well as* states for $k_x<0$ and $k_x\simeq 0$. This point is important and could help in understanding some recent results[12] obtained in the framework of CF theory. For the derivation of the electron and current density, we first calculated the Fermi energy E_F, taking into account that the number of electrons is constant. It turned out that although E_F is independent of k_x it is, however, a function of the magnetic field. This is due to the external confining potential. The electron and current densities show a very rich structure, which can be seen as a consequence of the quantization of the energy, although there is no simple relation between the k_x and y space, as is the case for a constant magnetic field. Moreover, the current density exhibits alternating ''channels'' of positive and negative current. It would be interesting too to include interaction between electrons and to study the effect of the self-consistency on the way the energy levels cross the Fermi energy. This can give rise to interesting phenomena, particularly in connection with the shape of the electron density.[8,13] Finally, because $\rho(y)$ is not constant, we have a contribution to the current density, directly due to the spin of the electron, which could imply some interesting phenomena in relation to spin polarized currents.

APPENDIX

Using the properties of the Hermite polynomial, the matrix elements H_{kn} can be derived in a recursive way. $\langle\phi_k|[(p_{\hat{y}}^2/2m')+a\hat{y}^4+b\hat{y}^3+c\hat{y}^2+d\hat{y}+e]|\phi_n\rangle$ gives
$n=k$:

$$\frac{1}{2m'}\left(\frac{1}{2}+k\right)+3a\left[k\left(1+\frac{(k-1)}{2}\right)+\frac{1}{4}\right]+c\left(\frac{1}{2}+k\right)+e,$$

$n=k+1$:

$$\left(\frac{(k+1)}{2}\right)^{1/2}\left(\frac{3b}{2}(1+k)\right),$$

$n=k+2$:

$$\left(\frac{(k+1)(k+2)}{4}\right)^{1/2}\left(-\frac{1}{2m'}+a(3+2k)+c\right),$$

$n=k+3$:

$$\left(\frac{(k+1)(k+2)(k+3)}{8}\right)^{1/2} b,$$

$n=k+4$:

$$\left(\frac{(k+1)(k+2)(k+3)(k+4)}{16}\right)^{1/2} a,$$

and $\langle\phi_n|V_c|\phi_m\rangle$, due to the confining potential,
$n=k$:

$$2\,\beta e^{-\alpha[1-(\alpha/4ye^2)]}L_k^0\left(-\frac{\alpha^2}{2ye^2}\right),$$

$n=k+i$:

$$\left[\beta e^{-\alpha[1-(\alpha/4ye^2]}\left(\frac{2^i}{n(n-1)\cdots(n-i+1)}\right)^{1/2}\left(\frac{\alpha}{2ye}\right)^i L_k^i \times\left(-\frac{\alpha^2}{2ye^2}\right)\right][1+(-1)^{2k+i}],$$

with L_n^{n-k} the associate Laguerre polynomial.

[1] For a review, see *The Quantum Hall Effect*, edited by E. Prange and S. M. Grivin (Springer, New York, 1987).
[2] For a review, see *Quantum Hall Effect*, edited by M. Stone (World Scientific, Singapore, 1992).
[3] J. E. Müller, Phys. Rev. Lett. **68**, 385 (1992).
[4] D. K. K. Lee, J. T. Chalker, and D. Y. K. Ko, Phys. Rev. B **50**, 5272 (1994).
[5] F. M. Peeters and A. Matulis, Phys. Rev. B **48**, 15 166 (1993); A. Matulis, F. M. Peeters, and P. Vasilopoulos, Phys. Rev. Lett. **72**, 1518 (1994); I. S. Ibrahim and F. M. Peeters, Phys. Rev. B **52**, 17 321 (1995).
[6] J. K. Jain, Phys. Rev. Lett. **63**, 199 (1989); Phys. Rev. B **41**, 7653 (1990).
[7] D. B. Chklovskii, Phys. Rev. B **51**, 9895 (1995); L. Brey, *ibid.* **50**, 11 861 (1994).
[8] D. B. Chklovskii, B. I. Shklovskii, and L. I. Glazman, Phys. Rev. B **46**, 4026 (1992).
[9] L. D. Landau and E. M Lifshitz, *Quantum Mechanics* (Pergamon Press, New York, 1977).
[10] C. L. Foden, M. L. Leadbeater, J. H. Burroughes, and M. Pepper, J. Phys. Condens. Matter **6**, L127 (1994); C. L. Foden, M. L. Leadbeater, and M. Pepper, Phys. Rev. B **52**, 8646 (1995).
[11] C. W. J. Beenakker, Phys. Rev. Lett. **68**, 385 (1990); A. M. Chang, Solid State Commun. **74**, 871 (1990).
[12] G. Kirczenow and B. L. Johnson, Phys. Rev. B **51**, 17 579 (1995).
[13] A. Shik, J. Phys. Condens. Matter **5**, 8963 (1993).